Atomic-Size Oscillations in Conductance Histograms for Gold Nanowires and the Influence of Work Hardening

I. K. Yanson,[1,2] O. I. Shklyarevskii,[1,3] Sz. Csonka,[4] H. van Kempen,[3] S. Speller,[3] A. I. Yanson,[2] and J. M. van Ruitenbeek[2]

[1]*B. Verkin Institute for Low Temperature Physics & Engineering, 47 Lenin Avenue, 61103, Kharkiv, Ukraine*
[2]*Kamerlingh Onnes Laboratorium, Universiteit Leiden, Niels Bohrweg 2, 2333 CA Leiden, The Netherlands*
[3]*Institute for Molecules and Materials, University of Nijmegen, Toernooiveld 1, 6525 ED Nijmegen, The Netherlands*
[4]*Electron Transport Research Group, Budapest University of Technology and Economics, 1111 Budapest, Hungary*

(Received 11 August 2005; published 16 December 2005)

Nanowires of different natures have been shown to self-assemble as a function of stress at the contact between two macroscopic metallic leads. Here we demonstrate for Au wires that the balance between various metastable nanowire configurations is influenced by the microstructure of the starting materials, and we discover a new set of periodic structures, which we interpret as due to the atomic discreteness of the contact size for the three principal crystal orientations.

DOI: 10.1103/PhysRevLett.95.256806 PACS numbers: 73.40.Jn, 61.46.+w, 68.65.La

Metallic nanowires have shown rich properties in terms of self-organization phenomena that are controlled by a combination of the quantum nature of the conduction electrons and the atomic-scale surface energy (see review [1] and references therein). Here we report yet another surprising series of stable structures.

At the very smallest scale the metals Au, Pt, and Ir spontaneously form into chains of atoms [2–4]. For slightly larger diameters further unusual arrangements referred to as ''weird wires'' were predicted [5] and later observed in high-resolution transmission electron microscopy (TEM) [6–8]. The observed structures for Au have a helical arrangement in the form of concentric shells of atoms.

In contrast to these atomic-packing driven structures, electronic shell filling has been shown to lead to an independent series of stable nanowire (NW) diameters for the free-electron-like alkali metals [9,10] and the noble metals [11–13]. These NWs were not imaged as in TEM, but their stability was inferred from frequently occurring stable conductance values during gentle breaking of the contacts (see below). The series of stable values has a characteristic period when plotted as a function of the square root of the conductance, $\sqrt{G}$, which is a measure of the radius of the wires.

Finally, regular bulk packing of NWs has also been observed, where the surface energy is the driving force, leading to completing of flat facets of the wires. Such effects have been observed in TEM [14–16] as remarkably long and stable wires, mostly for Au along the [110] direction. This atomic shell filling series has also been observed in the conductance [17], again as a regular period in $\sqrt{G}$.

Exactly which of these types of NWs self-assembles appears to depend critically on the experimental conditions, which is not fully understood. We anticipate that the selection of local minima in the free energy is influenced by the dynamics of the wire formation and the boundary conditions imposed by the structure of the leads. Here, we present evidence that the microstructure of the starting material, whether work hardened or annealed, influences the appearance of a new series of stable NWs that are periodic in the conductance, G, as opposed to $\sqrt{G}$ for the NWs observed previously.

Gold is the archetypal metal when investigating quantum transport phenomena in atomic-sized contacts [1]. The initial interest in these systems was in quantization of the conductance, in conjunction with the atomic discreteness of the contacts. The experimental technique frequently employed, which we also use here, involves the construction of histograms of conductance values from a large number of contact-breaking traces. The instrument used to adjust the contact size can be a scanning tunneling microscope or related piezocontrolled device. Here, we employ the mechanically controllable break junction technique. Briefly, it involves breaking a macroscopic wire of the metal under study at low temperatures under cryogenic vacuum. The clean fracture surfaces thus exposed are pushed back into contact, and finely controlled indentation-retraction cycles can be obtained through the action of a piezoelectric element. For a more detailed description we refer to [1].

The conduction histograms show the probability for observing a given conductance value G. For Au one typically observes a dominant peak in the histogram near $G = 1G_0$, where $G_0 = 2e^2/h$ is the conductance quantum. Further peaks are often found near $2G_0$, $3G_0$, and $4G_0$–$5G_0$, both at cryogenic and at room temperatures [18,19]. Slightly longer series of peaks, with small peaks near $G = 6$, and $7G_0$, have been reported [20], but these appear to be exceptional. Although many authors have presented this series of peaks as evidence for conductance quantization in Au, it has been pointed out many times that one cannot make a straightforward separation of genuine

electronic quantization effects from discreteness due to the atomic structure of the contacts [1,21]. It has now been generally accepted that the first peak results from a one-atom contact that also has a single conductance channel. The higher peaks are predominantly due to stable configurations of n atoms in cross section, with some quantization effects still observable [19,22].

For the results reported here the starting wire materials are work hardened Au wires, which is the key feature of our experiments. The original wires were obtained commercially [23], but the results have been reproduced by pulling similar wires at room temperature through a series of sapphire dies, reducing the diameter in small steps from 500 to 100 μm, without annealing the resulting wires. Using such wires, we repeatedly observe a periodic structure having up to 19 oscillations in the conductance range from 0 to $15G_0$ [Fig. 1(a)], with a distinct superstructure modulation. Note that the axis is broken and that the peak at $1G_0$ is about 5 times higher than the other peaks. The low-conductance part of the histogram is similar to those obtained in previous works on Au [18–20], except that the peaks near $3G_0$ and $4G_0$ are much stronger, and larger than the one at $2G_0$. The most striking feature is the large number of regularly spaced oscillations, having a pronounced amplitude modulation. Figure 1(b) emphasizes that the oscillations are periodic in G, not in $\sqrt{G}$. Figure 1(c) shows a Fourier transform of the spectrum in 1(a) between $1.2G_0$ and $15G_0$. We find two prominent "frequencies," at $f_1 = 1.4$ and $f_2 = 1.1G_0^{-1}$, that give rise to the beat minima near $2G_0$, $5G_0$, and $8G_0$. A smaller peak is visible at $f_3 = 0.8G_0^{-1}$. In order to see how the spectrum changes with the thinning of the NWs, we performed a Fourier transform for different parts of the original curve. When the neck is thick (for $G = 8G_0$–$15G_0$), only the f_1 periodicity is obtained. With further thinning the admixture of frequency f_2 starts to emerge until its amplitude approximately equals that of f_1. At the last stages just before arriving at a single-atom contact a hint of the f_3 periodicity appears.

Another important difference of the observed periodic structure in Fig. 1(a) with the atomic and electronic shell effects in NWs is the fact that the present features are observed at cryogenic temperatures, whereas shell effects are optimized by raising the temperature to a significant fraction of the melting point of the wires [12,13,17]. Figure 2(a) shows a histogram for the same work hardened Au wires recorded at room temperature. The histogram is very similar to previously reported data for Au at room temperature [18,24]. Some weak additional features are discernible above $5G_0$ that are not periodic in G and appear to be mostly due to the electronic shell structure; cf. [12,13]. After annealing of the wires at elevated temperatures, the usual Au conductance histograms for cryogenic temperatures [19,20] are recovered, as shown in Fig. 2(b). The amplitude modulation is absent, and the series of peaks terminates with very weak maxima at $6G_0$ or $7G_0$.

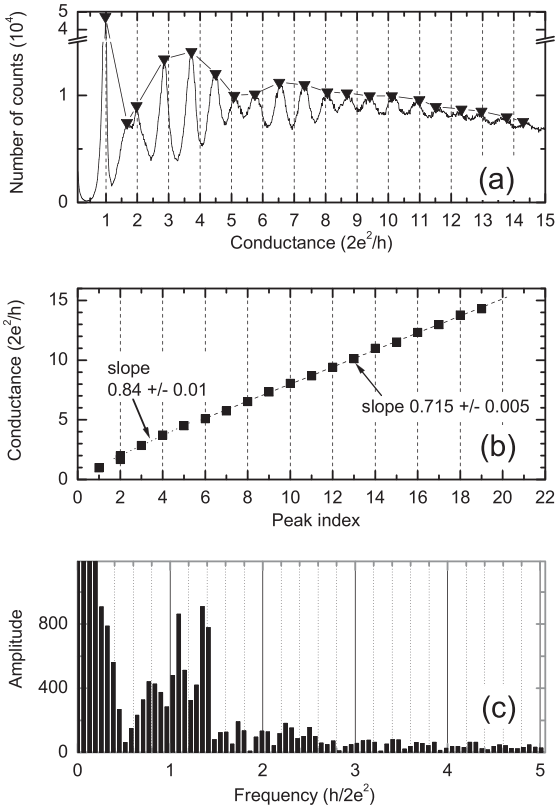

FIG. 1. Conductance histogram (a) obtained from 18 165 curves recorded while breaking the contact, using work hardened Au wires at $T = 6.5$ K, and at a bias voltage of 80 mV. The connected triangles show the position of oscillation maxima and emphasize the beating pattern. The positions of the maxima in the histogram are shown in (b) as a function of the index number, illustrating the periodicity. Linear fits are shown by dashed lines. (c) The components contributing to the beating pattern are obtained by a Fourier transform of the data in (a) between $1.2G_0$ and $15G_0$ so as to exclude the strong peak at $1G_0$. Three "frequencies" can be identified, ~0.8, 1.1, and $1.4G_0^{-1}$.

The difference in mechanical properties of the contacts for annealed and work hardened wires is also expressed in the global variation of the conductance with the stretching of the contact. In an essay that measures the length of stretching between the point at $G = 15G_0$ to the point of breaking over a large ensemble of contact indentation-breaking cycles, we observe that the mean length is about 80% *larger* for the work hardened wires. In contrast, the relative height of the first peak in the conductance histogram is suppressed for work hardened wires [Fig. 1 vs Fig. 2(b)], suggesting that chains of atoms are less readily formed.

The properties observed depend on the direction of motion of the electrodes. Figure 3 shows the comparison of direct and return conductance histograms for the same sample, which are recorded while stretching or indenting the contact, respectively. In the return histogram often (about 40% of the histograms recorded) the G-periodic

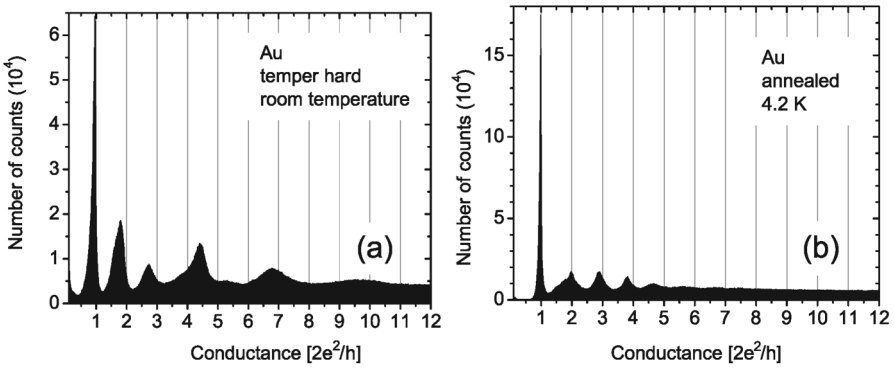

FIG. 2. Conductance histograms for work hardened Au wires (a) at room temperature, including 38 000 curves recorded at a bias voltage of 80 mV. (b) Conductance histogram obtained at 4.2 K after annealing the wires for 72 hours at 960 °C. The number of curves included is 15 000 and the bias voltage was 80 mV.

structure is replaced by a weak $\sqrt{G}$-periodic structure reminiscent of the electronic shell structure observed at room temperature [12,13].

Neither Cu nor Ag show a similar increase in the number of peaks for work hardened wires.

We now turn to a discussion of these results. In our interpretation we have been inspired by the results presented by Rodrigues *et al.* [16]. Their room temperature TEM images showed that Au NWs remain crystalline and fcc packed during stretching of the contacts, down to the last stage of thinning (see also Refs. [2,14,15]). The authors argue that NWs tend to form along the three principal crystallographic directions [100], [110], and [111]. Our key finding is that the observed periods in the conductance histograms may be explained by the atomic discreteness in the building of wires along the principal directions.

The conductance of a NW can be expressed in terms of its approximately circular cross-section area A as [1,25],

$$g = G/G_0 = \pi A - (\pi A)^{1/2} + 1/6, \qquad (1)$$

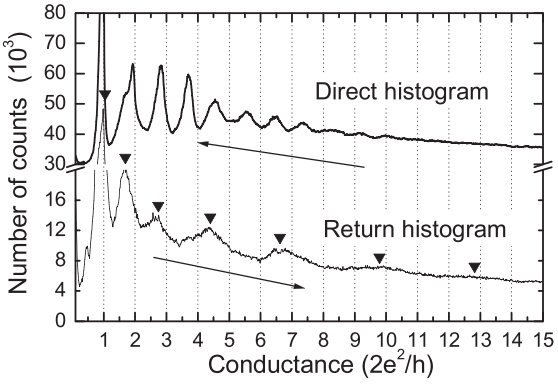

FIG. 3. Direct and return conductance histograms for a work hardened Au sample at $T = 6.5$ K. The direct histogram is shifted vertically for clarity. Arrows show the direction of recording of the conductance. Triangles show the positions of the maxima in the return histogram.

which is valid in the semiclassical limit. Here A is expressed in units of the Fermi wavelength square, λ_F^2 and the electrons are assumed to be confined by hard wall boundaries. If we take spill out of about $0.34\lambda_F$ beyond the boundaries into account by a slightly larger diameter [26], the correction nearly cancels the last two terms in Eq. (1). Therefore, we expect an approximately linear relation between g and A, $\Delta g \simeq \pi \Delta A$. For fcc packing in layers perpendicular to the three principal directions, [111], [100], and [110], one can identify two-dimensional unit cells comprising two Au atoms each. The area of the unit cells are $\frac{1}{2}\sqrt{3}a^2$, a^2, and $\sqrt{2}a^2$, respectively, where a is the lattice constant, $a = 4.08$ Å for bulk Au. Assuming the wire cross section is incremented by a single atom, the increment in conductance for the NW would scale roughly as $\Delta g_{111}/\Delta g_{100}/\Delta g_{110} = \frac{1}{2}\sqrt{3}/1/\sqrt{2} \cong 0.87/1/1.41$. This is close to the ratio of the periods, $1/f$, obtained from the experimental Fourier transform in Fig. 1(c). Quantitatively, along [100] the period would be $\Delta g_{100} = \pi(\frac{1}{2}a^2/\lambda_F^2) = (k_F a)^2/8\pi$. For a monovalent fcc metal $(k_F a)^3 = 12\pi^2$, giving $\Delta g_{100} = 0.96$, which is slightly larger than the experimental period $(G_0/f_2) = 0.91$. For the other two periods we obtain $\Delta g_{111} = 0.83$ and $\Delta g_{110} = 1.36$, compared to experimental values of $(G_0/f_1) = 0.71$ and $(G_0/f_3) = 1.25$. All experimental values are slightly smaller than expected from this simplified, clean free electron model. We tentatively attribute the reduction of the periods to a small overall reduction of the conductance due to scattering on defects near the contact, in analogy to similar corrections in the observation of electronic and atomic shell structure [9,17]. Further corrections may arise from relaxation of the atoms at the surface with respect to the fcc lattice positions.

We note that the relevant part of the NW at the smallest cross section is likely to be short, probably of order of a lattice spacing, a, in length. This may be deduced from the global shape of the conductance curves as a function of stretching. For regular wires at low temperatures the contact size decreases in steps about a single atom wide until

arriving at a single-atom contact. The work hardened wires stretch almost twice this length, making an average step width of about two lattice spacings. Yet, this is long enough for Eq. (1) to apply.

One of the most unexpected aspects of our results is the influence of work hardening of the starting materials, and the fact that this enhances the structure in the conductance histograms at low temperatures. The microstructure of the materials, in particular, the high density of grain boundaries may hold the answer to the question why this occurs. As is known for nanocrystalline materials (see, e.g., Ref. [27]), atoms at grain boundaries tend to flow under strain. This may provide enough freedom for the wires to adjust the local orientation of the grains on either side of the contact for optimal registry. At the same time there is not enough thermal activation energy available at cryogenic temperatures for atoms to diffuse over the surface and explore other metastable NW configurations, such as those determined by shell structure. The difference between stretching and compression of the contacts (Fig. 3) would follow in this interpretation from the difference between the stable equilibrium orientation of the two grains while pulling contrasted by the unstable configuration of two grains touching at an apex while being pushed into each other. For the latter we expect the grain orientations to be pushed away from alignment and a grain boundary to be introduced right at the contact point. The increased mobility of atoms at this grain boundary may give rise to a weak shell structure signal.

An extensive simulation of conductance histograms for Au nanocontacts has been reported by Dreher *et al.* [21]. They, indeed, find evidence for atomic discreteness in the histogram of contact cross sections, but this information is smeared out in the conductance histogram. Although this point deserves further study we speculate that the limited size of the repeat cell in the simulation may lead to enhanced disorder in the contact and a shorter NW length. This is partly visible in the width of the first conductance peak, which is much larger than in experiments.

This work is part of the research program of the ''Stichting FOM,'' partly sponsored through the SONS Programme of the European Science Foundation, which is also funded by the European Commission, Sixth Framework Programme, and was supported by the ''Nano'' program of the National Academy of Science of Ukraine under Project No. 10.05-H and by the Hungarian research funds OTKA TS049881. O. I. S. acknowledges a FOM visitor's grant.

[1] N. Agraït, A. Levy Yeyati, and J. M. van Ruitenbeek, Phys. Rep. **377**, 81 (2003).
[2] H. Ohnishi, Y. Kondo, and K. Takayanagi, Nature (London) **395**, 780 (1998).
[3] A. I. Yanson, G. Rubio Bollinger, H. E. van den Brom, N. Agraït, and J. M. van Ruitenbeek, Nature (London) **395**, 783 (1998).
[4] R. H. M. Smit, C. Untiedt, A. I. Yanson, and J. M. van Ruitenbeek, Phys. Rev. Lett. **87**, 266102 (2001).
[5] O. Gülseren, F. Ercolessi, and E. Tosatti, Phys. Rev. Lett. **80**, 3775 (1998).
[6] Y. Kondo and K. Takayanagi, Science **289**, 606 (2000).
[7] Y. Oshima, H. Koizumi, K. Mouri, H. Hirayama, K. Takayanagi, and Y. Kondo, Phys. Rev. B **65**, 121401 (2002).
[8] Y. Oshima, A. Onga, and K. Takayanagi, Phys. Rev. Lett. **91**, 205503 (2003).
[9] A. I. Yanson, I. K. Yanson, and J. M. van Ruitenbeek, Nature (London) **400**, 144 (1999).
[10] A. I. Yanson, I. K. Yanson, and J. M. van Ruitenbeek, Phys. Rev. Lett. **84**, 5832 (2000).
[11] E. Medina, M. Díaz, N. León, C. Guerrero, A. Hasmy, P. A. Serena, and J. L. Costa-Krämer, Phys. Rev. Lett. **91**, 026802 (2003).
[12] A. I. Mares, A. F. Otte, L. G. Soukiassian, R. H. M. Smit, and J. M. van Ruitenbeek, Phys. Rev. B **70**, 073401 (2004).
[13] A. I. Mares and J. M. van Ruitenbeek, Phys. Rev. B **72**, 205402 (2005).
[14] Y. Kondo and K. Takayanagi, Phys. Rev. Lett. **79**, 3455 (1997).
[15] T. Kizuka, Phys. Rev. Lett. **81**, 4448 (1998).
[16] V. Rodrigues, T. Fuhrer, and D. Ugarte, Phys. Rev. Lett. **85**, 4124 (2000).
[17] A. I. Yanson, I. K. Yanson, and J. M. van Ruitenbeek, Phys. Rev. Lett. **87**, 216805 (2001).
[18] M. Brandbyge, J. Schiøtz, M. R. Sørensen, P. Stoltze, K. W. Jacobsen, J. K. Nørskov, L. Olesen, E. Lægsgaard, I. Stensgaard, and F. Besenbacher, Phys. Rev. B **52**, 8499 (1995).
[19] B. Ludoph, M. H. Devoret, D. Esteve, C. Urbina, and J. M. van Ruitenbeek, Phys. Rev. Lett. **82**, 1530 (1999).
[20] J. L. Costa-Krämer, N. García, and H. Olin, Phys. Rev. B **55**, 12 910 (1997).
[21] M. Dreher, F. Pauly, J. Heurich, J. C. Cuevas, E. Scheer, and P. Nielaba, Phys. Rev. B **72**, 075435 (2005).
[22] H. E. van den Brom and J. M. van Ruitenbeek, Phys. Rev. Lett. **82**, 1526 (1999).
[23] Gold wire, 75 μm diameter, ''temper hard,'' Advent Research Materials Ltd., Catalogue No. 518609.
[24] J. L. Costa-Krämer, Phys. Rev. B **55**, R4875 (1997).
[25] J. A. Torres, J. I. Pascual, and J. J. Sáenz, Phys. Rev. B **49**, 16 581 (1994).
[26] J. M. van Ruitenbeek, M. H. Devoret, D. Esteve, and C. Urbina, Phys. Rev. B **56**, 12 566 (1997).
[27] D. Wolf, V. Yamakov, S. R. Phillpot, A. Mukherjee, and H. Gleiter, Acta Mater. **53**, 1 (2005).